Parameter estimation for grey-box models of building thermal behaviour

O. M. Brastein [a,*], D.W.U. Perera [a], C. Pfeifer [a], N.-O. Skeie [a]

[a] *Department of Electrical engineering, Information Technology and Cybernetics, University Collage of Southeast Norway, 3918 Porsgrunn, Norway*

Energy and Buildings, 2019, 169, 58-68.
DOI: https://doi.org/10.1016/j.enbuild.2018.03.057

Abstract

Good models for building thermal behaviour are an important part of developing building energy management systems that are capable of reducing energy consumption for space heating through model predictive control. A popular approach to modelling the temperature variations of buildings is grey-box models based on lumped parameter thermal networks. By creating simplified models and calibrating their parameters from measurement data, the resulting model is both accurate and shows good generalisation capabilities. Often, parameters of such models are assumed to be a combination of different physical attributes of the building, hence they have some physical interpretation. In this paper, we investigate the dispersion of parameter estimates by use of randomisation. We show that there is significant dispersion in the parameter estimates when using randomised initial conditions for a numerical optimisation algorithm. Further, we claim that in order to assign a physical interpretation to grey-box model parameters, we require the estimated parameters to converge independently of the initial conditions and different datasets. Despite the dispersion of estimated parameters, the prediction capability of calibrated grey-box models is demonstrated by validating the models on independent data. This shows that the models are usable in a model predictive control system.

Keywords: Grey-box models, parameter estimation, Monte Carlo methods, thermal network model, dispersion of estimated parameters

*Corresponding author: Tel: +47 47 45 05 69

E-mail address: ole.m.brastein@usn.no

This research did not receive any specific grant from funding agencies in the public, commercial, or not-for-profit sectors.

1 Introduction

A large part of the world's energy production is used for heating and cooling buildings. The fraction of total energy production consumed for utilities in commercial and residential buildings has been estimated at 32% by the International Energy Agency (IEA), according to [1]. Even though modern building techniques are able to reduce the energy used for heating, the renewal rate of buildings is low. Berthou et al. [2] reports renewal rates of 1% per year in France. This illustrates the need for good building energy management systems (BEMS) in existing buildings as well.

A model predictive control (MPC) system is an attractive solution for use in a BEMS. Models of building thermal behaviour can be used to predict the heating and cooling time of a building. In a MPC system, a model is used to simulate the system ahead in time in order to find a sequence of inputs that controls the system to the desired state. In a BEMS, the use of MPC will allow for improved tracking of the temperature setpoint as well as minimization the energy consumption [2, 3]. Predictions of future system inputs are readily available from weather forecasts, which helps to facilitate the use of MPC.

There have been several publications studying the use of MPC for building thermal control. In [4] the authors use both active heating and passive solar blinds to control indoor air temperature. The paper also gives a thorough introduction to the various MPC control methods, such as deterministic and stochastic MPC. In [5] a complete building model is developed as a set of layered models and used in an MPC. The authors report an energy saving of 63% in thermal energy and 29% in HVAC electric energy, for a four-month test period. These examples show the potential benefits of using MPC for building thermal control. They also show the importance of a good prediction model for MPC to be feasible.

There are a number of different modeling approaches that can be used to model the thermal behaviour of a building in an MPC system [6]. In Perera et al. [1], a white-box model based on mass and energy balance is derived and calibrated for specific buildings. This type of model gives a set of ordinary and/or partial differential equations (ODE/PDE) that must be discretised and solved. For complex models, a large number of parameters are required that can be difficult to identify. Another approach to modelling is the use of black-box models, which relies solely on measurement data without any prior knowledge of the building, e.g. ARMAX [7, 8] or PLS-R [9, 10] models. These types of models show high prediction accuracy, but do not usually allow the application of physical knowledge to define the model. This approach also produces models with low generalisation between different buildings, which makes building-to-building comparisons of models difficult [11]. Comparing the thermal behaviour of buildings can be of interest for the purposes of energy consumption classification.

Another approach to modelling thermal behaviour of buildings is the use of grey-box models [2, 3, 12, 13]. A grey-box model is based on a simplified structure derived from a cognitive understanding of the physics involved. For the heating of buildings, the model structures may consist of thermal networks [14], i.e. resistor-capacitor circuit equivalent lumped parameter models. Rather than deriving the full model as in [1], the simplified model structure is developed from an understanding of the heat transfers involved in a building, which provides directly a reduced order model. This process can be referred to as 'cognitive' model development [14]. The parameters of such models are lumped parameters, i.e. each parameter represents a combination of multiple physical quantities. Such parameters must be identified from measurement data, since they are generally difficult to compute based on technical building specifications. A grey-box model therefore uses a combination of the white- and black-box approaches [15].

It is often assumed that the parameters of such models can be assigned physical meaning. The identified parameters are compared to the physical properties of the building [16, 17]. For interpretation of model parameters to be justified, we suggest that the results of the parameter estimation process must show a low degree of dispersion, e.g. be independent of the initial guess parameter vector for the estimation algorithms. Estimation of parameters is required to give similar results when using different datasets from the same building.

The estimation of parameters requires the measurement data to contain enough dynamic information about the system to accurately calibrate the model [16, 18-20]. Since the subject of this work is physical buildings, the experimental design is challenging. The outdoor weather conditions acts as a model input, particularly the outdoor temperature. Further, it is of interest to estimate the parameters under realistic conditions for an occupied building. Hence the choice of excitation of the system is limited. Lack of dynamic information in the data is known to give problems with practical identifiably [19].

Since all the parameters of a grey-box model must be estimated, an additional challenge with calibrating grey-box model parameters is over-parameterisation [16]. This is known to give non-convergent parameter estimates, since an over-parameterised model has undetermined optimal parameters, i.e. infinitely many solutions exist.

While challenges caused by practical identifiably and/or over-parameterisation may give reason to question the physical interpretation of the estimated parameters the models may still be usable in an MPC. In this work, the dispersion of parameter estimates under different experimental conditions is investigated using multiple sets of experimental data from a real building. Further, calibrated models are validated on indepenant data to show that they are capable of predicating the thermal behaviour of the test building, hence rendering them usable in an MPC system.

2 Model, methods and measurements

A common approach to parameter estimation is the use of numerical optimisation [19], either directly [2] or in the form of a maximum likelihood (ML) method [17, 21]. When using numerical optimisation, it is of interest to investigate the dispersion in the estimated optimal parameters under different experimental conditions. In particular, it is interesting to study if the initial guess for the optimisation affects the estimated parameters.

2.1 Model and parameters

The model used in this paper is a thermal network model of a building [3, 14, 16, 17, 20, 22], presented using an electrical circuit equivalent model. Thermal resistance is modelled as resistors and thermal capacitance as capacitors. The resulting model is a circuit where the temperature is used as the driving potential, and the flow through the circuit is the heat flow. This approach has been used in a number of published papers on modelling building thermal behaviour, e.g. [3, 13].

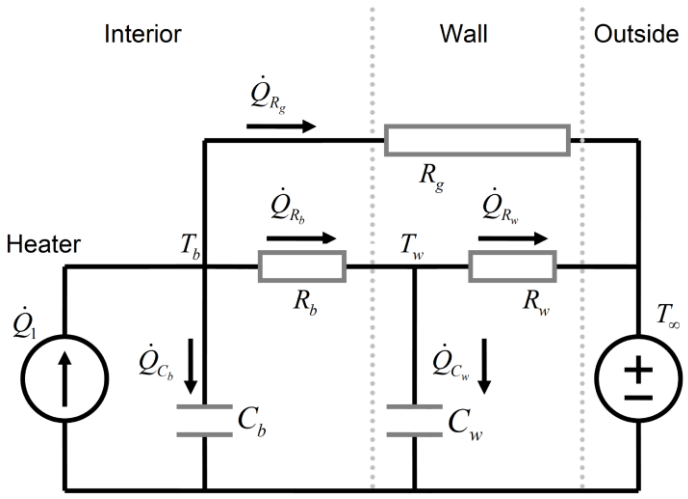

Figure 1 - The R3C2 thermal network model

The focus of this paper is estimation of the model parameters. For simplicity, only one model is investigated, and the model structure is chosen as a minimalistic representation of the experimental building from which the calibration data is collected. The model is shown in Figure 1. This model is similar to the R3C2 model used in [2], but the resistance for ventilation is removed since there is no ventilation system installed in the test building.

The model consists of two states T_b and T_w, which correspond to the interior temperature of the building and the wall temperature respectively. Wall temperature is measured on the inner surface of the wall. For each state there is an associated capacitance, C_b and C_w. These capacitances represent

the building's ability to store thermal energy in the interior and the building envelope, e.g. walls, floor and ceiling. The remaining three model components are resistances. R_b represents the thermal resistance between the building interior and the wall. R_w is the resistance to heat flow through the wall, i.e. between the state T_w and the outside temperature. The third resistance R_g represents the resistance to heat flow through the parts of the building envelope that are not included in the state T_w, such as windows and the door. The driving forces of the system are $\dot{Q}$ and T_∞, where $\dot{Q}$ is a heat flow source, e.g. an electric heater. The outside temperature is modelled as a potential source T_∞.

Deriving equations from a thermal network model can be done with, for example, Kirchhoff's node potential law [23, 24]. Each state in the circuit, T_b and T_w, is assigned to a circuit node and the flow into and out of each node is balanced. The model can be written in state-space form as a set of ordinary differential equations (ODEs) [18]:

$$\frac{dT_b}{dt} = -\left(\frac{1}{C_b R_b} + \frac{1}{C_b R_g}\right) T_b + \left(\frac{1}{C_b R_b}\right) T_w + \left(\frac{1}{C_b}\right) \dot{Q}_1 + \left(\frac{1}{C_b R_g}\right) T_\infty \tag{1}$$

$$\frac{dT_w}{dt} = \left(\frac{1}{C_w R_b}\right) T_b - \left(\frac{1}{C_w R_w}\right) T_w + \left(\frac{1}{C_w R_w}\right) T_\infty \tag{2}$$

The parameter vector is then defined as:

$$\theta = \begin{bmatrix} R_g & R_b & R_w & C_b & C_w \end{bmatrix}^T \tag{3}$$

The output from the model is the states themselves, and both states are directly measurable. The measurement equations are therefore found by including the measurement noise terms v_b and v_w with the system states:

$$\begin{aligned} y_{T_b} &= T_b + v_b \\ y_{T_w} &= T_w + v_w \end{aligned} \tag{4}$$

The measurement noise v_b and v_w is assumed zero mean Gaussian with standard deviation r_b and r_w:

$$v_b \sim N(0, r_b) \quad , \quad v_w \sim N(0, r_w) \tag{5}$$

Both measurements are temperatures from the same Data Acquisition (DAQ) system, hence it is reasonable to expect that they have similar noise characteristics. This is verified by computing the standard deviation for both measurements over a range of measurements where the temperatures are approximately constant.

2.2 Deterministic approach to parameter estimation

The state transition equations in the model are an approximation of the real system. Hence, there will be some unknown influence from modelling errors in the simulations. The state transition

equations in eq. 1 and 2 are written as ODE's. These could be extended to a set of stochastic differential equations (SDE) by the addition of a process noise term w [20]. The probability density function (pdf) of the process noise term w is not easily obtained, however it is often assumed Gaussian. This assumption can be checked during model validation [20, 21] by use of e.g. autocorrelation to verify that the residuals are indeed white noise This method can confirm the assumption of Gaussian process noise [20]. While the use of SDE's is a more statistically solid approach [16, 17, 20, 21], it is also possible to treat the estimation problem as deterministic without the process noise term w [6, 25]. The model is then a set of deterministic ODE's. This reduces the estimation of model parameters to a least squares curve fitting problem which can be solved directly by numerical optimization [2]. In this work, the deterministic curve fitting approach is used.

2.3 Parameter ranges and nominal values

A nominal parameter vector is used as a starting point for the estimation methods. These parameter values are based on trial and error experiments, together with prior knowledge of the approximate range where reasonable values may be obtained. The physical insight required as a starting point for these trial and error experiments is limited to the approximate order of magnitude of the parameters. It is assumed that this can be obtained for most practical buildings. It is not required that the nominal values themselves give a good prediction model for the building, only that they are approximately in the correct range. They are mainly used as normalisation constants, such that parameter estimation can be performed in unit scale, and to restrict the search space to a region of interest where reasonable parameter values may be obtained.

Table 1 – Nominal parameter values and min./max. range

	Rg [K/W]	R_b [K/W]	R_w [K/W]	C_b [J/K]	C_w [J/K]
Nom. value (θ_0)	0.160	0.060	0.100	1200k	1200k
Min. (θ_{min})	0.048	0.018	0.03	360k	360k
Max. (θ_{max})	0.272	0.102	0.170	2040k	2040k

Table 1 gives a summary of the nominal parameter values with min./max. ranges used for the R3C2 model. The nominal values are chosen such that any region of interest in the parameter space is contained within +/-70% of each nominal value. Hence $\theta_{min} = 0.3 * \theta_0$ and $\theta_{max} = 1.7 * \theta_0$. In the following, discussions on the estimation of parameters and the shape of the objective function in parameter space are valid only within the ranges specified in Table 1.

2.4 Numerical optimisation

The subject of numerical optimisation used for parameter identification is covered in literature, e.g. [2, 19, 26]. Optimisation algorithms are used to find a minimum point of an objective function. In parameter estimation, this objective function is typically the model fit, i.e. the square error over a set of reference data compared to model simulations. In this work, the simulation error is computed over the whole calibration period, rather than using the one-step ahead prediction errors traditionally used in statistics [8, 20]. This results in a least squares curve fitting approach to parameter estimation, as discussed in section 2.2. This gives the objective function as the mean square error (MSE) between simulated and measured temperatures computed over the whole dataset. A standard quadratic norm [18] is chosen as the error function, i.e.:

$$J = \sum_{i=1}^{N}\sum_{k=1}^{nx} e_k^2 = \sum_{i=1}^{N}\sum_{k=1}^{nx}\left(T_k^i - T_k^{i,ref}\right)^2 \tag{6}$$

$$RMSE = \sqrt{\frac{J}{nx \cdot N}} \tag{7}$$

Here, nx is the number of states (temperatures) and N is the number of samples in the dataset. The sum of squared error of each of the two temperature states is added together and the errors of all states are weighted equally. An alternative approach is to weight the errors by their uncertainty, e.g. the covariance of the measurements, as is typically done in the statistical approach to parameter estimation [20]. Since the temperatures are measured by the same DAQ system it is reasonable to assume similar uncertainty in both measurements and hence use equal weights on the error for both states. All samples in the calibration data Z^N are assumed to have equal uncertainty, such that the weighting of the errors is also uniform in time.

To simplify the evaluation of results, the objective score J is divided by the number of samples and the square root taken, thus giving the root mean square error (RMSE). This quantity has the same unit (℃) as the states. The optimisation algorithm works directly on the sum of square error objective J.

The optimisation algorithm of choice in this paper is the Constrained Optimization BY Linear Approximation (COBYLA), which was developed by M.J.D. Powell [26]. The implementation is taken from the Accord.Net project [27]. There are two important settings of the algorithm, RhoEnd and MaxIttr. The first controls the accuracy of the optimised variables, while the second is a loop break to ensure the algorithm completes even if no optimal solution is found. In this project, RhoEnd is set to 1e-4 and MaxIttr is 1e4. This allows COBYLA to find the solution with sufficient accuracy. In all following cases, the algorithm completes without reaching the maximum number of iterations.

2.5 Experimental setup and data

The building of interest in this paper is an experimental setup built in 2014 at the campus of University College of Southeast Norway, in Porsgrunn [28].

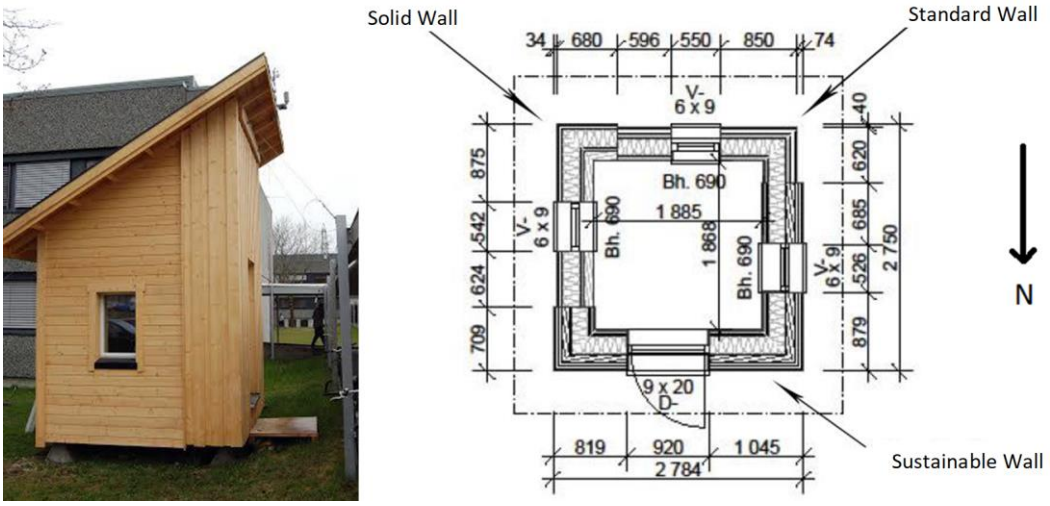

Figure 2 - A view of the experimental building with floorplan

Figure 2 shows a view of the test building from the outside, together with the floor plan. This building has support structures made out of concrete so it is not in contact with the ground. The inner volume is approximately 9.4 m3 and sealed such that neither natural ventilation nor mechanical ventilation is provided. The building has three small windows of each 60x90 cm2, one in each of the south, east and west directions, and a door of 90x120 cm2 in the north direction. Three buildings surrounding the experimental building limit the solar irradiation through the windows.

The building envelope is constructed using layers of diverse materials, including wooden cladding, glass wool, air fill, polyethylene vapour barriers, wood, cement chipboard, particleboard and cardboard. There are three different types of walls each having unique construction by compounding different materials stated above. Roof and floor of the building also have different composition in each.

The experimental building has an electrical heater of 375W consisting of a thermostat controller, a measurement system, and a logging computer that uses approximately 100W. The measurement system consists of sensors for measuring the inside and outside temperatures and humidity, air pressures, rainfall, and wind speed and wind direction, and total power usage. The power usage is logged every 10 seconds, the temperatures and humidity are logged every 10 minutes, and the weather data is logged every 30 minutes. All data is stored in CSV (Comma Separated Values) files. The temperature sensors are mostly of the silicon type (TMP 36) with an accuracy of +/- 1 ℃. Data was collected using multiple data from these CSV files, and pre-processed. During the pre-processing steps the data was filtered, combined and re-sampled by linear interpolation. This gives a combined dataset

where all the variables of Z_N are known at the same time instants t_i, regardless of the initial sampling times for the different CSV files. In the final dataset, a sampling time of dt=10 minutes is used.

Measurement data was collected from the building during November and December 2015. Since buildings are exposed to weather, experimental design options are limited. This poses a challenge in ensuring that the calibration data contains sufficient dynamic information for parameter estimation. If buildings are occupied, this poses further restrictions on the experimental design. The data used here is derived from an empty building, but under realistic experimental conditions, i.e. exposed to weather and other unmeasured disturbances.

Since the window area exposed to solar irradiation is limited and the data was collected during the winter in Norway, heat gain from solar irradiation is assumed negligible. Hence, in order to limit the model complexity, the solar irradiation is not included in the dataset or the model.

Table 2 - List of datasets

Dataset name	Start time	End time	Length [h]	N
Nov1	02.11.2015 17.18.00	10.11.2015 00.08.00	175	1050
Nov2	10.11.2015 00.18.00	17.11.2015 07.08.00	175	1050
Dec1	04.12.2015 18.00.00	11.12.2015 08.50.00	159	954
Dec2	11.12.2015 19.40.00	17.12.2015 00.00.00	124.5	747

A list of four datasets, including identifying names, is given in Table 2. Estimation of parameters, i.e. fitting a model structure to a particular physical system, requires information about that system in the form of a set of measurements Z^N [18]. This set contains both reference data in the form of system outputs y and information about the excitations for the system in the form of system inputs u, i.e.:

$$Z^N = \{y_1, u_1, y_2, u_2, ..., y_N, u_N\} \quad (8)$$

If the states are directly measurable, as is the case with building temperatures, the outputs are simply equal to the states with the addition of measurement noise. The measured states y_i in Z^N are temperatures T_b and T_w. The inputs u_i consist of the outside temperature T_∞ and power consumption $\dot{Q}$ of the building.

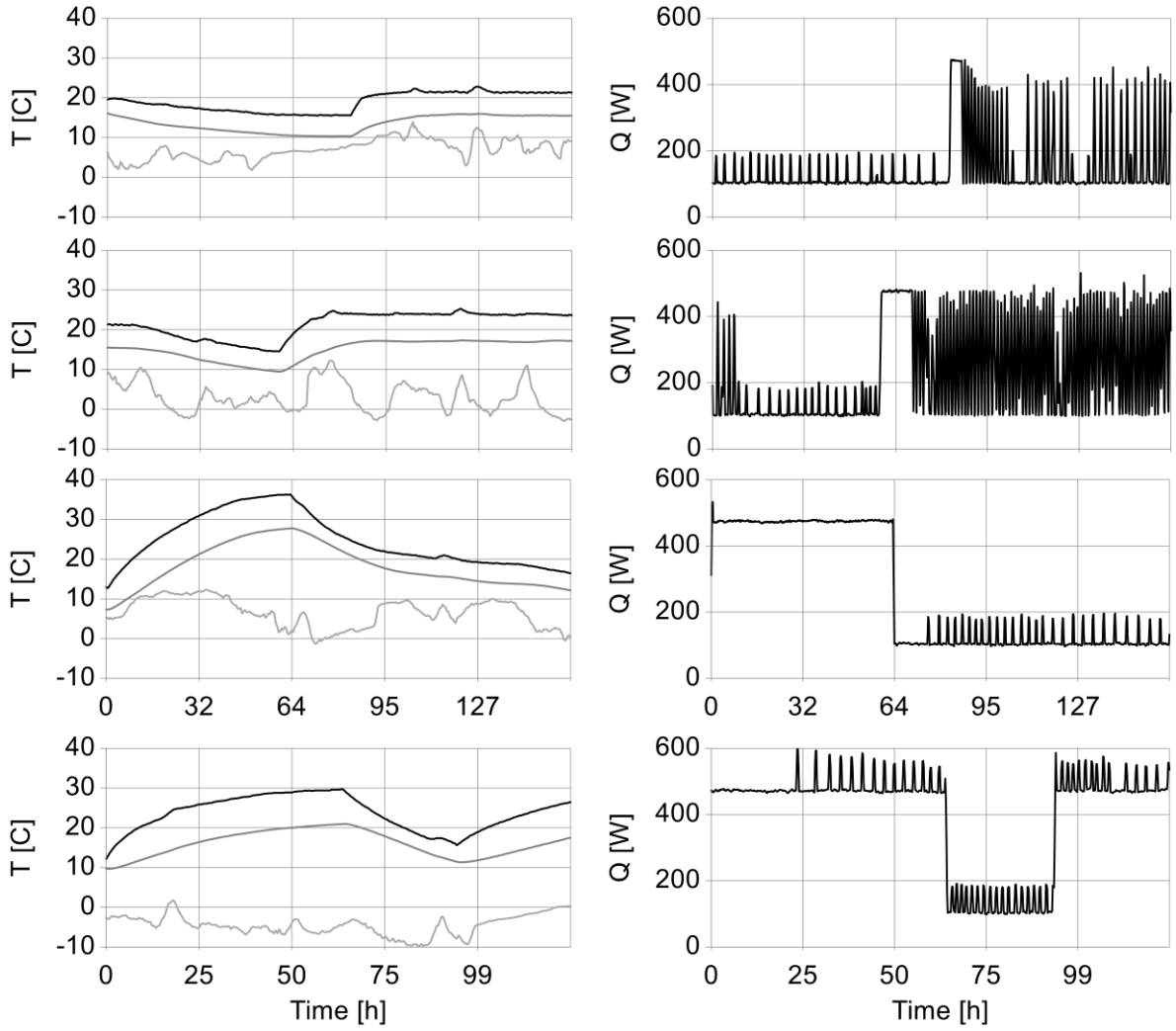

Figure 3 - Plots of all datasets. On the left side, temperatures for building interior T_b (black), building wall T_w (grey) and outdoor temperature T_∞ (light grey) are shown. On the right side, the power consumed in the building is plotted (black). The datasets Nov1, Nov2, Dec1 and Dec2 are plotted from top to bottom respectively.

The contents of each of the four datasets are plotted in Figure 3. These datasets were generated by introducing arbitrarily chosen steps in the thermostat setting of the electric heater in order to simulate realistic variations in setpoint for a building in use. While this approach may be inferior to, for instance, a pseudo random binary sequence (PRBS) [22], it is more realistic since it mimics temperature changes of a building in use. Changing temperature setpoints from a low to a high setting (approximate step sizes of 10°C to 20°C are used here) takes a significant time, typically around 12–48 hours. This is reflected in the slow response to the step in supplied power, shown in the plots of data.

A constant minimum power consumption of about 100W is observed in Figure 3. This power is consumed by computer equipment used for data logging in the test facility. When the on/off thermostat control turns the heater on, an additional 350W of power is drawn by the heater.

When the heater is regulating the temperature at a setpoint requiring less than full capacity (<100% on-time), there are spikes in the power consumption data caused by the thermostat switching the heater on and off. These spikes are present in the November data, but not in the December data. In November, the heater was set at a maintainable temperature setting of approximately 25°C, i.e. the system is under on/off control. In December, the heater setpoint was turned to maximum, which is higher than the achievable temperature at full power under the given experimental conditions. Hence, the heater was constantly on for long periods of time.

For the parameter estimation, all the supplied power is included in $\dot{Q}$. Hence the input to the model is taken directly from the data as shown here. This is a simplification, since some power is consumed by other equipment in the building. However, it is assumed that all the supplied energy is converted to heat, either by the electric heater or the other equipment. For simplicity, the total heat generation from all appliances is denoted as a single heater.

3 Results

The R3C2 model is based on the physical structure of a building and the parameters are estimated using measurement data. The thermal parameters of buildings are assumed to be time invariant. Hence, it is expected that there exists a single, true, parameter vector for the grey-box model determined by the physical properties of the building. Convergence of parameter estimates towards such a parameter vector can be considered a requirement for physical interpretation of the final model. The results presented here are computed mainly from the *Nov1* dataset.

The denomination *degrees of freedom* (DOF) is used to describe the number of free parameters in the estimation problem. The R3C2 model has five parameters, constituting five DOF.

3.1 Maximum degrees of freedom, five estimated parameters

The first method used to investigate the parameter space of the model is a simple Monte Carlo approach. In the following results, M = 50000 simulations of the model are executed. Model parameters are randomly and independently drawn from the range $\theta_{min} \leq \theta \leq \theta_{max}$, given in Table 1. This is similar to a simple random search, except that we are interested in the collection of all results, not just the one with the lowest RMSE. The resulting plots consist of points, one for each simulation, which gives a view of the shape of the objective function J in parameter space. The abscissa of the plots represents parameter values and the ordinate axis represents the resulting root mean square error (RMSE) for each simulation.

In this section, all five parameters of the R3C2 model are free, i.e. they are estimated as opposed to kept constant.

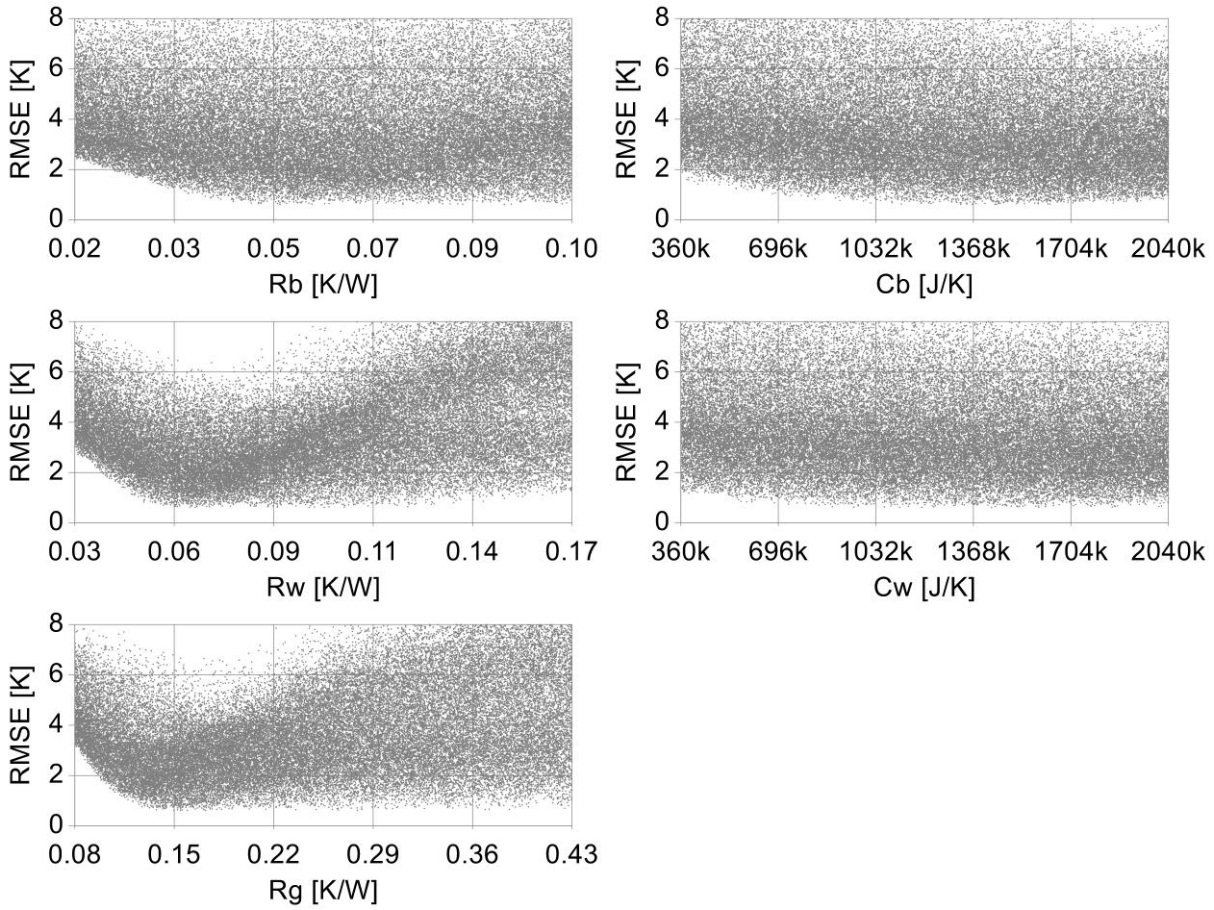

Figure 4 - Monte Carlo simulations with 5 degrees of freedom. This figure shows the resulting scatter plots for the parameters.

As shown in Figure 4, most of the randomly drawn parameter vectors are not optimal since the RMSE is higher then the minimum. However, some solutions fall close to the minimum RMSE of 0.591°C for the R3C2 model and Nov1 dataset. When all five parameters are estimated, the objective function is flat in the minimum RMSE region. Since there is no clear minimum, the estimated parameter from an optimisation algorithm will not converge to a single parameter vector but rather produce vectors in an optimal range, all with the same minimum RMSE.

The next method is also based on Monte Carlo (MC) simulations. Randomly drawn parameters are used as the initial guess of a numerical optimisation algorithm (COBYLA). The initial guess and the subsequent parameter estimate are plotted for all iterations of the optimisation algorithm. The points are interconnected by a line in order to identify which particular initial guess corresponds to each solution. Each plot consists of 50 iterations, i.e. repeated randomised initial guesses followed by execution of the optimisation algorithm.

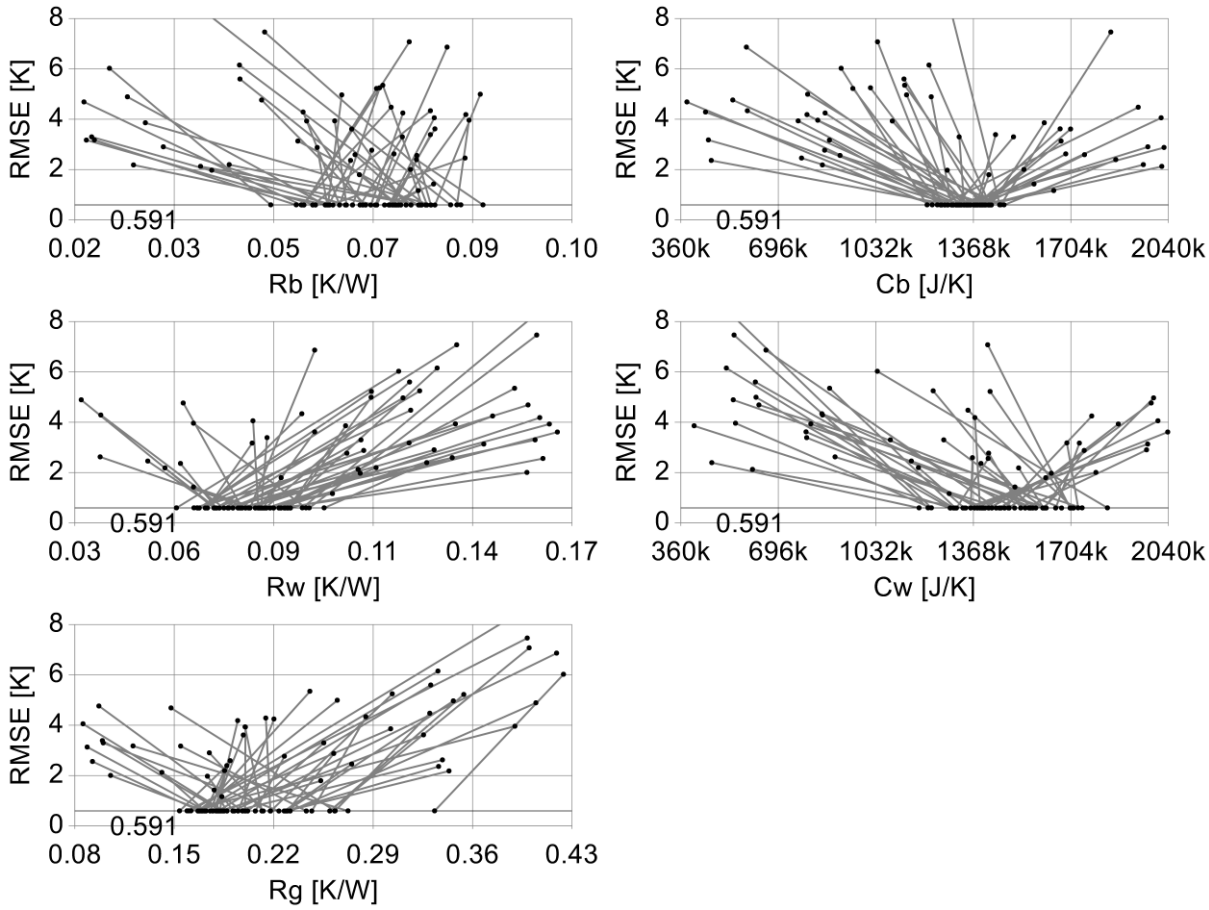

Figure 5 - Randomised initial guess and estimated solution is plotted together. This figure shows the results of applying the bespoke method to the R3C2 model simulated in the Nov1 dataset.

As shown in Figure 5, the optimisation algorithm finds optimal solutions, i.e. RMSE ~ 0.6°C, from all 50 starting points, but the resulting optimal solution varies significantly with the initial guess. The parameter estimates do not converge. Based on the plots in Figure 4, this is expected. Figure 5 further shows that the RMSE objective function is flat around the minima, since many equally good solutions exist for a large range of parameter values.

3.2 Reduced degrees of freedom, 4 free parameter

As discussed, we expect the estimated parameters to converge towards a true, physically determined, parameter vector. Since the results so far indicate that this is not the case, an explanation for the dispersion in parameter estimates is needed.

Over-parameterization [16], i.e. too many degrees of freedom (DOF) in the estimation problem, is one plausible explanation for the observed flatness of the objective function. The DOF is reduced by fixing one parameter at a constant value, thus reducing the number of free parameters to estimate. Reduction in freedom is only applied to the estimation problem, by the reduction of free variables, and

does not affect the model structure. All five parameters are used in the simulations and the model remains the same.

The parameter chosen to be kept as constant is R_g. This parameter represents the thermal resistance of windows and doors, i.e. the part of the building envelope directly exposed to both interior and exterior temperatures. Because R_g represents doors and windows, which usually have known 'UA' values [1], it is assumed that R_g would be the easiest to compute based on building technical specifications. UA values are computed as the product of U and A, where U is the reciprocal of thermal resistance per area and A is the area. Hence, knowing R or U for all windows and doors, as well as their area A allows for computation of $R_g = 1 / (U_g A_g)$.

Table 3 - Building specification according to manufacturer of windows and door

	U [W/m²K]	A [m²]	UA [W/K]	R [K/W]
Door	1.2	1.76	2.1	0.48
Windows	1.3	1.57	2.0	0.50
Total	-	-	4.1	0.24

As shown in Table 3, the specifications give a theoretical R_g of 0.24. However, this includes only one door and three windows. Comparing the R3C2 model to the building, R_g is also expected to include any other element of the building that gives a direct influence between outside temperature and indoor air temperature without affecting the wall temperature. Hence, the theoretical R_g can be considered an upper bound of the true Rg, as any contribution by remaining building elements can only lower R_g. Note therefore that it is considered acceptable that the theoretical R_g is in the upper region of the nominal range defined in Table 1.

First, the parameter space for the reduced DOF case is observed by using MC simulation of parameter space.

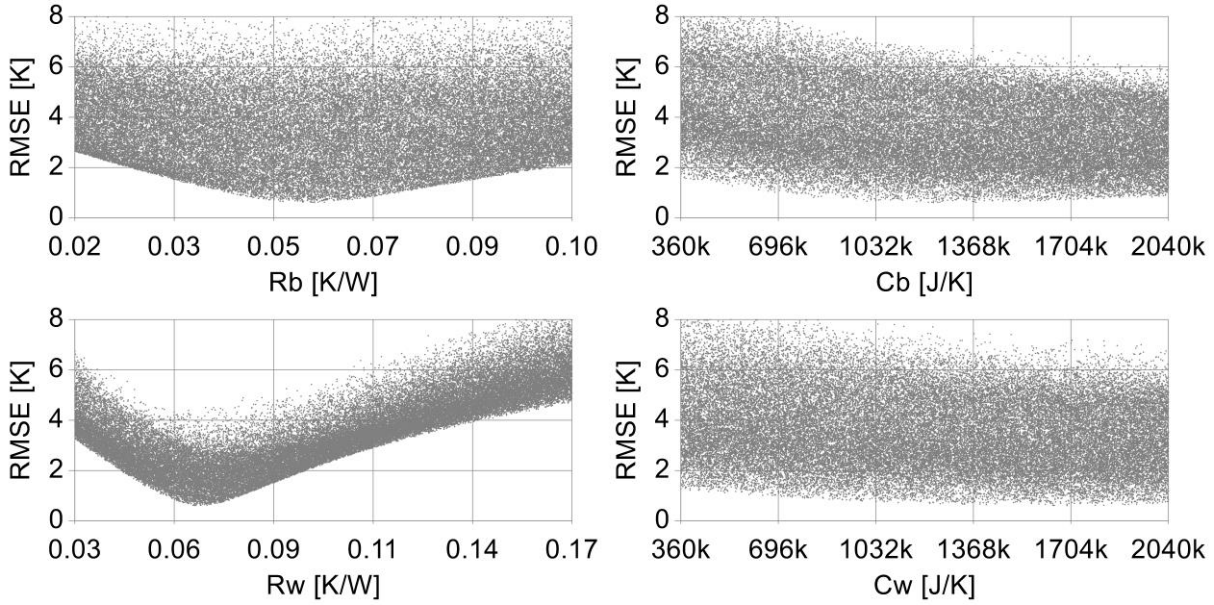

Figure 6 - Scatter plots of MC simulation in parameter space. This figure shows the results of applying MC simulation of the parameter space to the R3C2 model simulated on the Nov1 dataset, with a fixed parameter Rg = 0.24 [K/W].

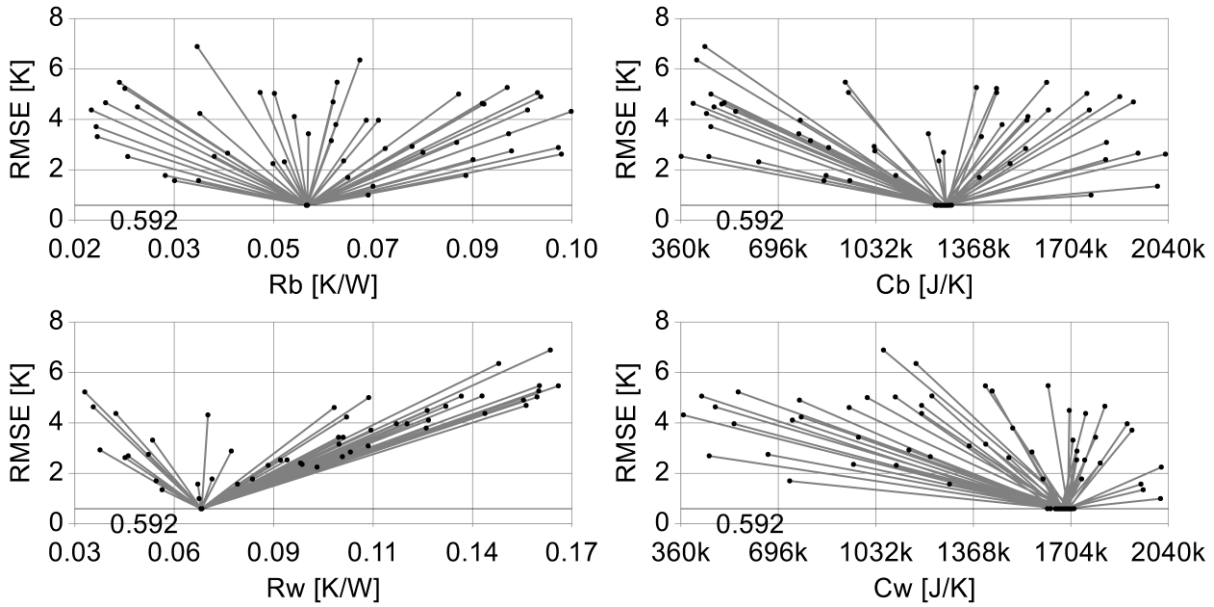

Figure 7 - Randomised initial guess and optimal solution is plotted together. This figure shows the results of applying the bespoke method to the R3C2 model simulated on the Nov1 dataset. With reduced freedom in the estimation problem, the trajectories of the optimsation now show a distinct convergent pattern, independent of the initial random guess.

As shown in Figure 6, the MC simulations of the parameter space now show a significantly different shape of the objective function, which now has a well defined minimum. Subsequently, optimisation is now expected to converge towards a single parameter vector.

Comparing Figure 7 with Figure 5, it is evident that the dispersion in estimated parameters is significantly decreased. Based on the MC simulations of parameter space shown in Figure 6, it is reasonable to conclude that the objective function has more pronounced minima when one DOF is eliminated from the estimation problem. With a distinctly convex objective function, the optimiser is able to find the same optimal solution independent of initial guess.

Multimodal objective functions are a typical challenge of numerical optimisation. This has not been discussed here, since the plots from the MC method are used to show that the objective function is either flat or unimodal in the region of interest.

3.3 Quantitative comparison of results from DOF reduction

In order to quantitatively compare the cases presented in sections 3.1 and 3.2, the standard deviation (SD) of estimated parameter values is computed.

Table 4 – Sample standard deviation of parameter estimates, as a percentage of nominal value

	R_g [%]	R_b [%]	R_w [%]	C_b [%]	C_w [%]
5 DOF	19.23	14.43	10.05	5.093	12.18
4 DOF	-	0.066	0.079	1.230	2.208

Table 4 lists the SD as a percentage of the nominal value, as a measure of the dispersion of estimated parameters from both the cases with five and four DOF. By reducing the number of free parameters, the dispersion of the parameter estimates is significantly reduced, in particular for the resistance parameters. Slightly more variation is observed in the two capacitance parameters.

3.4 Comparing results from multiple datasets

Until now, all results are taken from a single dataset, Nov1. As demonstrated, too many DOF will lead to a flat objective function, which in turn gives a large dispersion in estimated parameters. Next, it is of interest to introduce more data to the parameter estimation, namely the datasets Nov2, Dec1 and Dec2. Thermal building behaviour parameters are assumed to change slowly with time, unless modifications to the building structure are introduced. For the datasets presented in section 2.5, no such modifications occurred. Hence, it is reasonable to assume that the parameter estimation methods will give similar results for the four datasets.

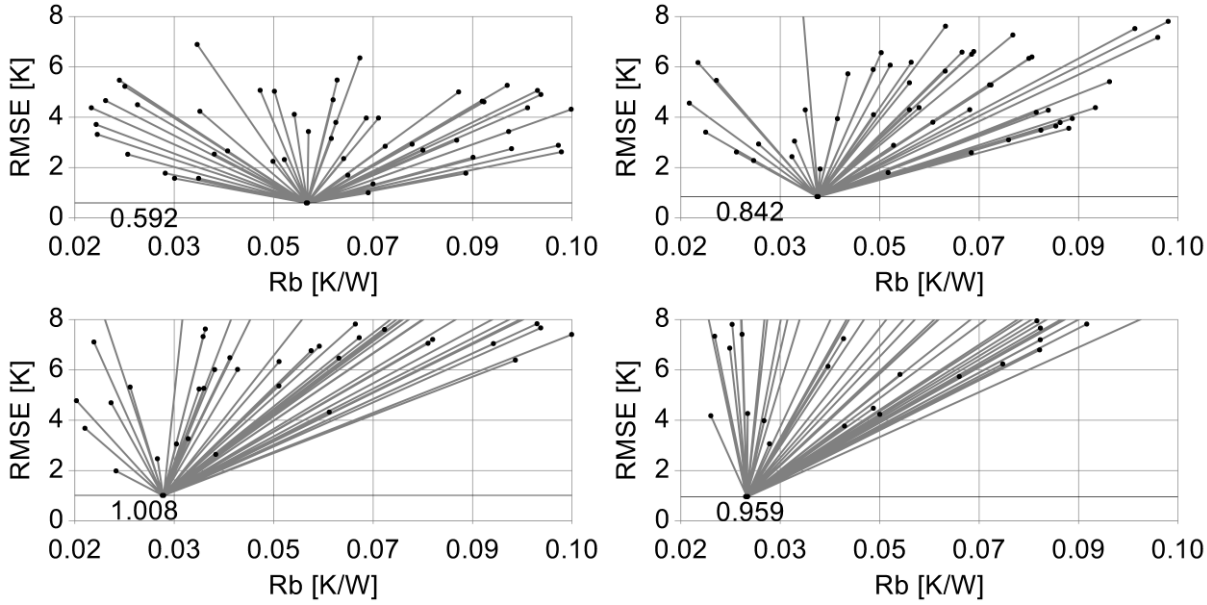

Figure 8 - Comparing optimisation results and convergence for R_b over four datasets. The top left plot is for Nov1, top right for Nov 2, lower left for Dec1 and lower right for Dec2.

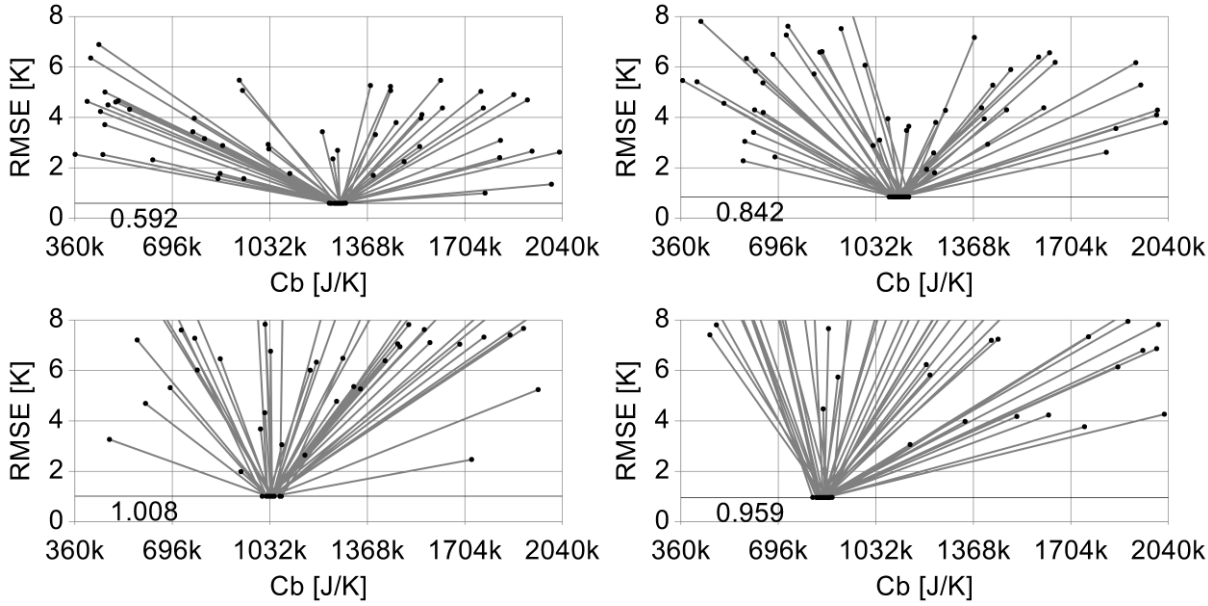

Figure 9 – Comparing optimisation results and convergence for C_b over all four parameter sets. The top left plot is for Nov1, top right for Nov 2, lower left for Dec1 and lower right for Dec2.

Figure 8 shows the plots from randomised initial guess to estimated parameter for the parameter R_b estimated on all four datasets using the four DOF model. As previously demonstrated for dataset Nov1, the parameter estimates converge independently of the initial guess per iteration of the method. This also holds for the other three datasets. However, the parameter value that gives minimum RMSE is different for each dataset, i.e. the solution for each dataset is not the same parameter vector.

Figure 9 shows the results for the parameter C_b. The plots show that the estimated parameter values for C_b also vary between the four datasets, same as for R_b, although this variation is smaller for C_b than R_b. Similar results are obtained for the other two parameters. Next, it is useful to quantitatively compare the estimated parameter values and their corresponding variance, for all four datasets.

Table 5 - Summary of average parameter estimates for all four datasets

Dataset	R_b [K/W]	R_w [K/W]	C_b [J/K]	C_w [J/K]	RMSE4 [K]	RMSE5 [K]
Nov1	0.057	0.066	1271k	1673k	0.592	0.591
Nov2	0.041	0.079	1107k	1321k	0.842	0.835
Dec1	0.033	0.072	1033k	1529k	1.008	1.010
Dec2	0.029	0.087	852k	1241k	0.959	0.963

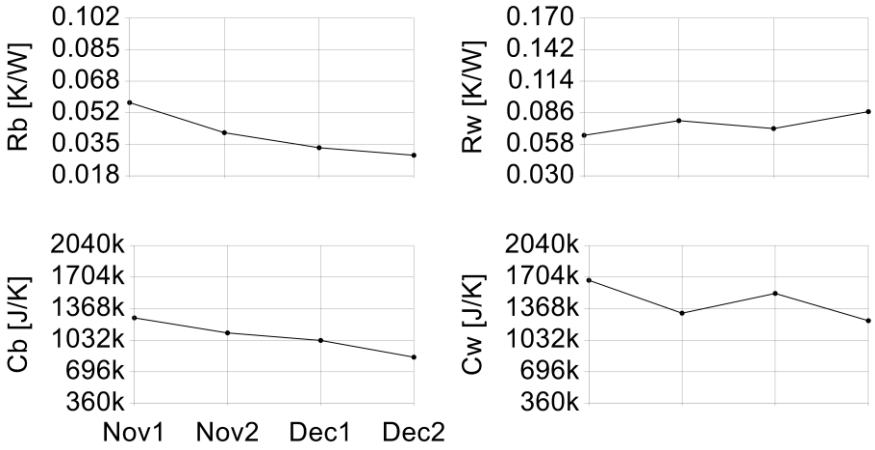

Figure 10 – Estimated parameters for each dataset

Estimated values for each parameter for all datasets are given in Table 5 and plotted in Figure 10. Columns RMSE4 and RMSE5 give the root mean square error (RMSE) of the simulations using estimated parameter vectors, from four and five DOF cases respectively. There are significant variations in the estimated parameters when comparing multiple datasets, e.g. R_b for Nov1 is twice as large as for Dec1 and Dec2. It is unlikely that the thermal resistance between room interior temperature and wall temperature is halved in just four weeks. As such, these variations are probably not caused by physical effects. A plausible explanation is insufficient dynamic information content in the data. As discussed, this can lead to problems with practical identifiably [19].

An important observation from Table 5 is the similarity between RMSE values for the five and four DOF cases, as shown in the two last columns. While fixing R_g to a constant value – thereby removing it from the parameter estimation problem – decreases the dispersion of estimated parameters, this does not affect the final RMSE of the model with estimated parameters.

Table 6 - Summary of parameter estimates' sample standard deviation for all four datasets

Dataset	R_b [%]	R_w [%]	C_b [%]	C_w [%]
Nov1	0.065	0.079	1.230	2.208
Nov2	0.079	0.027	1.252	1.995
Dec1	0.066	0.070	0.854	1.250
Dec2	0.105	0.027	1.078	2.144

The standard deviation of parameter estimates, as a percentage of nominal values, is given in Table 6. As shown, the dispersion of parameter estimates is similar for all four datasets, even though the estimated parameter values are different. These results could indicate that the spread of the parameter estimates is problem specific, independent of the datasets, while the actual value of each parameter depends on the calibration data.

3.5 Model validation

In order to show that the identified model parameters could be used for predicting the thermal behaviour of the building, it is required to validate the model using new data, independent of the data used for parameter estimation. So far, the results are based on model fit, i.e. how well the model is able to fit a particular set of data. A superior measure of model accuracy is the models ability to predict the thermal behaviour using a new dataset. This validates the model performance in similar conditions as those of a Model Predictive Control (MPC) system. Hence it gives a good indication of the models performance used for the purpose of controlling the building temperature. The results in this section are based on the four DOF model.

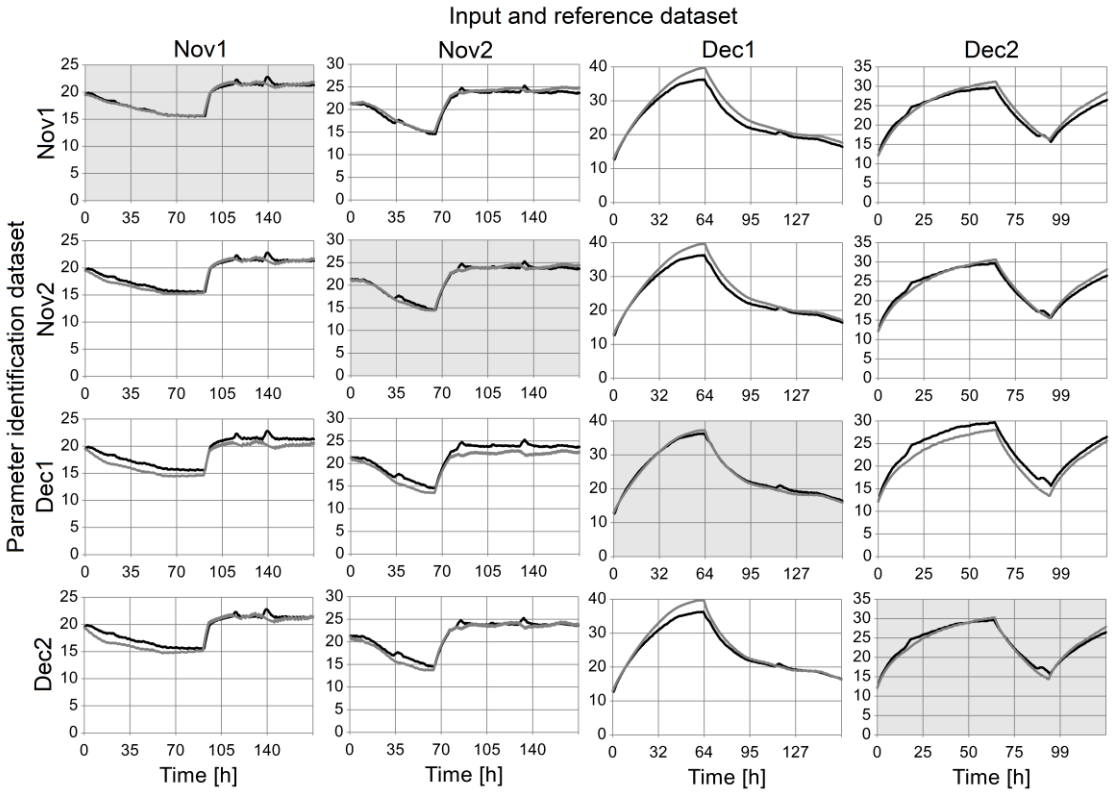

Figure 11 - Results from model simulation are plotted for all four datasets using the four parameter sets shown in Table 5. The results on the diagonal of this figure are model fit results, while the off-diagonal elements are validation results. For the validation plots the parameters are estimated using a dataset that is independent from the one used for inputs and measurement references. The model fit results are plotted on grey background to separate them from the validation results. The simulation results are plotted in grey while the reference data are plotted in black.

The results for T_b from validating the model are shown in Figure 11. The columns represent the dataset used for validation while the rows show the dataset used for parameter estimation. This gives that the diagonal plots are model fit result, while the off-diagonal elements are model validation results. The model fit results on the diagonal are plotted on grey background to separate them from the validation results, and are included in the figure for comparison with validation results. The measured temperatures are plotted in black, and the simulated in gray.

Table 7 - Simulation errors (RMSE) in T_b for all four datasets and parameter sets

Identification dataset	Input and reference dataset			
	Nov1	Nov2	Dec1	Dec2
Nov1	0.330	0.596	1.899	1.174
Nov2	0.562	0.513	1.692	0.861
Dec1	1.247	1.463	0.588	1.803
Dec2	0.936	0.857	1.586	0.807

Table 8 - Simulation errors (RMSE) in T_w for all four datasets and parameter sets

Identification dataset	Input and reference dataset			
	Nov1	Nov2	Dec1	Dec2

Nov1	0.492	2.095	2.494	5.605
Nov2	1.326	0.668	1.119	2.528
Dec1	1.068	0.833	0.822	2.958
Dec2	2.155	1.471	2.460	0.526

The RMSE results for all 16 combinations of dataset and parameter sets are given in Table 7 and Table 8. These results, together with the plots in Figure 11, show that the model is capable of giving good prediction accuracy also for unknown data, although the RMSE varies for different combinations. As for Figure 11, the diagonal elements on grey background are the model fit results, while off-diagonal elements in both tables are results from validating the model on independent data. The prediction error for T_b is around 0.5°C to 1.5°C for most cases, with some combinations approaching 2°C. Considering that MPC uses feedback, model prediction errors around 1C is likely adequate for the intended purpose. As evident from Table 8 the errors are significantly larger for T_w. However, in a building energy management system, it would be the interior temperature T_b that is of importance for the controller.

4 Discussion

It could be argued that physical interpretation of grey-box parameters for a building model requires that the parameter estimates converge towards a single point in parameter space. If the parameter estimates show a large dispersion in their description of a predominantly time-invariant physical system, they cannot be directly correlated to the specific physical properties of the building.

However, the model as a whole may still be able to accurately predict the behaviour of the system, even if the parameters cannot be assigned a physical interpretation. This is illustrated in the model validation in section 3.5. The calibrated models where shown to give mean square errors of prediction of around 0.5°C to 1.5°C for a ~7 day test period for the internal building temperature T_b. Models with prediction errors of this magnitude may be considered usable in MPC systems.

Despite acceptable model validation results, it is of interest to study the reasons for the observed dispersion of estimated parameters, since this gives reason to question the physical interpretability of the estimated parameters. The use of Monte Carlo (MC) sampling of parameter space together with scatter plots of the resulting root mean square error (RMSE) from simulations compared to measurement data was shown to provide a view of the objective function in parameter space. This allows visualisation of the convexity of the objective function, which in turn facilitates cognitive evaluation of the expected optimisation algorithm behaviour.

A randomised initial starting point and repeated execution of optimisation algorithms were used to show that the optimal solution can depend on the starting point. Further, this dispersion in

estimated parameters was shown to depend to some extent on the degrees of freedom (DOF) in the estimation problem, since reducing the DOF in the estimation decreases the dispersion of estimated parameters.

Despite reducing the number of estimated parameters, the results still do not converge to a single parameter vector when multiple calibration datasets are used. It is plausible that the datasets used in this work do not contain sufficient dynamic information to identify the model parameters. It is well known that lack of dynamic information in calibration data, caused by insufficient excitation of the physical system during data acquisition, may give rise to problems of practical identifiably [16, 18, 19]. Due to the experimental conditions encountered when collecting data on building thermal behaviour, ensuring that data contain sufficient dynamic information can be challenging.

Another possible explanation for the observed behaviour of the parameters is that the simplicity of the model allows the estimation procedure to use model parameters to account for unmodeled effects in the physical system. Unknown disturbances, such as variations in humidity or wind, may not be similar between the four investigated datasets.

5 Conclusion

The use of multiple datasets for parameter estimation, as well as the use of MC methods, was shown to give insight into the dispersion of estimated parameters. The model with identified parameters was further shown to give good predictions of building thermal behaviour, and as such would be suitable for model predictive control. However, if physical interpretation of individual parameters is of interest, the dispersion in the parameter estimates needs to be eliminated. This can be done by addressing the challenges of practical identifiably through improved excitation of the physical system. Further, the over-parameterisation of the grey-box model can be reduced by limiting the number of free parameters in the estimation problem.

6 References

[1] D. W. U. Perera, C. F. Pfeiffer, and N.-O. Skeie, "Modelling the heat dynamics of a residential building unit: Application to Norwegian buildings," *Modeling, Identification and Control,* vol. 35, pp. 43-57, 2014.

[2] T. Berthou, P. Stabat, R. Salvazet, and D. Marchio, "Development and validation of a gray box model to predict thermal behavior of occupied office buildings," *Energy and Buildings,* vol. 74, pp. 91-100, 5// 2014.

[3] S. F. Fux, A. Ashouri, M. J. Benz, and L. Guzzella, "EKF based self-adaptive thermal model for a passive house," *Energy and Buildings,* vol. 68, Part C, pp. 811-817, 1// 2014.

[4] F. Oldewurtel, A. Parisio, C. N. Jones, D. Gyalistras, M. Gwerder, V. Stauch*, et al.*, "Use of model predictive control and weather forecasts for energy efficient building climate control," *Energy and Buildings,* vol. 45, pp. 15-27, 2012/02/01/ 2012.

[5] T. Hilliard, L. Swan, and Z. Qin, "Experimental implementation of whole building MPC with zone based thermal comfort adjustments," *Building and Environment,* vol. 125, pp. 326-338, 2017/11/15/ 2017.
[6] S. Prívara, J. Cigler, Z. Váňa, F. Oldewurtel, C. Sagerschnig, and E. Žáčeková, "Building modeling as a crucial part for building predictive control," *Energy and Buildings,* vol. 56, pp. 8-22, 2013/01/01/ 2013.
[7] L. Ljung, "Prediction error estimation methods," *Circuits, Systems and Signal Processing,* vol. 21, pp. 11-21, 2002/01/01 2002.
[8] M. J. Jiménez, H. Madsen, and K. K. Andersen, "Identification of the main thermal characteristics of building components using MATLAB," *Building and Environment,* vol. 43, pp. 170-180, 2// 2008.
[9] K. Esbensen, *Multivariate analysis in practice*. Oslo: CAMO, 1998.
[10] D. W. U. Perera, M. Halstensen, and N.-O. Skeie, "Prediction of Space Heating Energy Consumption in Cabins Based on Multivariate Regression Modelling," *International Journal of Modeling and Optimization,* vol. 5, 2015.
[11] A. Afram and F. Janabi-Sharifi, "Review of modeling methods for HVAC systems," *Applied Thermal Engineering,* vol. 67, pp. 507-519, 6// 2014.
[12] A. Afram and F. Janabi-Sharifi, "Gray-box modeling and validation of residential HVAC system for control system design," *Applied Energy,* vol. 137, pp. 134-150, 1/1/ 2015.
[13] G. Reynders, J. Diriken, and D. Saelens, "Quality of grey-box models and identified parameters as function of the accuracy of input and observation signals," *Energy and Buildings,* vol. 82, pp. 263-274, 10// 2014.
[14] K. K. Associates, *Thermal Network Modeling Handbook*, 2000.
[15] M. J. Jiménez, H. Madsen, J. J. Bloem, and B. Dammann, "Estimation of non-linear continuous time models for the heat exchange dynamics of building integrated photovoltaic modules," *Energy and Buildings,* vol. 40, pp. 157-167, // 2008.
[16] H. Madsen and J. Holst, "Estimation of continuous-time models for the heat dynamics of a building," *Energy and Buildings,* vol. 22, pp. 67-79, 3// 1995.
[17] N. R. Kristensen, H. Madsen, and S. B. Jørgensen, "Parameter estimation in stochastic grey-box models," *Automatica,* vol. 40, pp. 225-237, 2// 2004.
[18] L. Ljung, *System identification - Theory for the user*. Upper Saddle River, NJ 07458: Prentice Hall PTR, 1999.
[19] R. Johansson, *System modeling and identification*. Englewood Cliffs: Prentice Hall, 2012.
[20] P. Bacher and H. Madsen, "Identifying suitable models for the heat dynamics of buildings," *Energy and Buildings,* vol. 43, pp. 1511-1522, 7// 2011.
[21] N. R. Kristensen and H. Madsen, *Continuous Time Stochastic Modelling, CTSM 2.3 - Mathematcs Guide*: Technical University of Denmark, 2013.
[22] K. K. Andersen, H. Madsen, and L. H. Hansen, "Modelling the heat dynamics of a building using stochastic differential equations," *Energy and Buildings,* vol. 31, pp. 13-24, 1// 2000.
[23] J. W. Nilsson and S. A. Riedel, *Electric Circuits*, 6th ed.: Prentice Hall, 2001.
[24] T. L. Floyd, *Electronic devices*. Upper Saddle River, N.J.: Prentice Hall, 2002.
[25] C. Verhelst, F. Logist, J. Van Impe, and L. Helsen, "Study of the optimal control problem formulation for modulating air-to-water heat pumps connected to a residential floor heating system," *Energy and Buildings,* vol. 45, pp. 43-53, 2012/02/01/ 2012.
[26] M. J. D. Powell, "A Direct Search Optimization Method That Models the Objective and Constraint Functions by Linear Interpolation," in *Advances in Optimization and Numerical Analysis*, S. Gomez and J.-P. Hennart, Eds., ed Dordrecht: Springer Netherlands, 1994, pp. 51-67.
[27] C. R. Souza, "The Accord.NET Framework," ed. Sao Carlos, Brazil, 2014.
[28] D. Perera and N.-O. Skeie, "Estimation of the Heating Time of Small-Scale Buildings Using Dynamic Models," *Buildings,* vol. 6, p. 10, 2016.